Available online at www.sciencedirect.com

Journal of Catalysis 220 (2003) 172–181

JOURNAL OF CATALYSIS

www.elsevier.com/locate/jcat

Solid-state chemistry of ammonium and cesium 1-vanado-11-molybdophosphate and ammonium 12-molybdosilicate: application to oxidation catalysis

N. Laronze,* C. Marchal-Roch, N. Guillou, F.X. Liu, and G. Hervé

Institut de Réactivité, Electrochimie et Microporosités, UMR 8637, Université de Versailles, 45 Avenue des Etats-Unis, 78035 Versailles cedex, France

Received 24 February 2003; revised 16 May 2003; accepted 16 May 2003

Abstract

The solid-state behavior of $(NH_4)_4[PMo_{11}V^VO_{40}]$, crystallized from a water/dioxane solution, has been studied. Decomposition of one of the four ammonium cations occurs easily and a thermal treatment in air at 220 °C leads to $(NH_4)_3H[PMo_{11}VO_{40}]$. Further ammonium decomposition was observed between 220 and 300 °C up to $(NH_4)_{0.8}H_{3.2}[PMo_{11}VO_{40}]$. Only one cubic phase was evident and the lattice parameter increases as ammonia is eliminated. Rietveld refinement of X-ray patterns of all samples is better with an occupancy of $\frac{3}{4}$ for anionic sites, as previously proposed for $Cs_4[PMo_{11}VO_{40}]$. Solid-state substitution of cesium for ammonium cations has been performed by thermal treatments at 300 °C of the ammonium salt impregnated by cesium nitrate. Only three ammonium cations can be substituted. The catalytic behavior of these salts for the oxidative dehydrogenation of isobutyric acid reveals high catalytic activity and selectivity to methacrylic acid for all the samples up to three cesium cations but fall down hereafter.

Keywords: Catalysis; Heteropolyanion; Ammonium vanadomolybdophosphate; Isobutyric acid oxidation

1. Introduction

Heteropolymolybdates have been widely used for oxidation of organic molecules such as alcohols, aldehydes, isobutyric acid, and alkanes. By a control of the molecular composition of the heteropolyanion, it is possible to fine tune its acid and oxidizing properties. The nature of the cation influences also the crystallographic lattice, the texture, the thermal stability, and also the acid and redox behaviors of the heteropolysalts [1]. Therefore, complicated formulas which combine alkaline cations (K, Cs), transition metals (V, Cu, Fe, Ni, Mn), and main group metals (Sn, Sb, As) have been often proposed in many patents or more fundamental studies [2,3].

Acidic cesium salts of the 1-vanado-11-molybdophosphoric acid have attracted much attention since the presence of vanadium increases the catalytic activity and cesium has been reported to increase both the stability and the reoxidation rate of the catalyst [4]. For isobutyric acid (IBA) oxidative dehydrogenation, Lee et al. determined an optimum of methacrylic acid (MAA) formation for $x = 2.75$ in the series of $Cs_xH_{4-x}PMo_{11}VO_{40}$ salts at 350 °C [5]. Above $x = 3.5$, no more methacrylic acid was formed. In the case of isobutane oxidation, Mizuno et al. also observed a maximum yield in MAA and methacrolein for $x = 2.5$ in the series $Cs_xH_{3-x}PMo_{12}O_{40}$ or $Cs_xH_{3.84-x}Ni_{0.08}PMo_{11}VO_{40}$ at 340 °C [6,7]. These results have been interpreted by the enhancement of surface acidity and surface-oxidizing ability of cesium salts with less than 3 Cs per heteropolyanion. Nevertheless, in some cases, the true molecular composition and the structure of the catalysts have been poorly characterized both initially and at the steady state [1,5,6,8,9]. In situ, as well as ex situ characterizations of acids and partially salified heteropolyacids have been performed for the oxidation of methacrolein and isobutyric acid. It was shown that vanadium [10–13] and molybdenum [14,15] migrate from the heteropolyanion to the crystal lattice under the reaction conditions and are probably present as cationic oxospecies.

In previous studies, we have demonstrated that solid solutions of mixed ammonium–cesium salts of $[PMo_{12}O_{40}]^{3-}$ can be obtained by solid-state exchange [16]. The study has been extended to more active compounds which contain

---

* Corresponding author.
E-mail address: laronze@chimie.uvsq.fr (N. Laronze).

0021-9517/$ – see front matter © 2003 Elsevier Inc. All rights reserved.
doi:10.1016/S0021-9517(03)00242-2

vanadium, derived from $(NH_4)_5[PMo_{11}V^{IV}O_{40}]$ [17]. The thermal behavior of this salt showed that a phase, isostructural of the cubic phase of $(NH_4)_3[PMo_{12}O_{40}]$, was obtained after a thermal treatment at 210 °C and was stable up to 410 °C. Moreover, solid solutions containing NH_4^+ and Cs^+ cations can be obtained up to only three cations for an heteropolyanion [18]. The same limitation to three cesium cations has been observed by Lee et al. when cesium is substituted for protons in $H_4[PMo_{11}VO_{40}]$. On the contrary, cubic salts $Cs_xH_{4-x}[PMo_{11}VO_{40}]$, with $0 \leqslant x \leqslant 4$, have been described in a recent study of Berndt et al. [19], which propose a general explanation of their cubic structure according to the cationic composition.

The aim of this work was to prepare well-defined stoichiometric ammonium and cesium 1-vanado(V)-11-molybdophosphates, in order to study their structure and their thermal behavior. They were compared to those of $(NH_4)_4[SiMo_{12}O_{40}]$, an isostructural and isocharge compound without vanadium.

Moreover, mixed ammonium–cesium salts obtained by solid-state Cs^+/NH_4^+ exchange with $(NH_4)_4[PMo_{11}V^VO_{40}]$ have been prepared and characterized in order to determine the influence of the initial oxidation state of vanadium on the reactivity for the catalytic oxidative dehydrogenation of isobutyric acid.

2. Experimental

2.1. Preparations

$(NH_4)_4[PMo_{11}V^VO_{40}]$ was obtained in two steps, first synthesis of the 1-vanado(V)-11-molybdophosphoric acid $H_4[PMo_{11}V^VO_{40}]$ as previously described [20], and then neutralization of this acid. The heteropolyacid $H_4[PMo_{11}V^VO_{40}]$ was dissolved in water/dioxane v/v (0.36 mol L^{-1}), and then solid ammonium hydrogenocarbonate was added up to a rapid increase of pH until pH $\approx$ 4 (pH meter previously calibrated in water). Orange crystals of $(NH_4)_4[PMo_{11}V^VO_{40}]$ were obtained from the solution placed at 4 °C. This ammonium salt was heated at 120 °C for 24 h in air flow in order to eliminate dioxane. The solid was rehydrated at room temperature. Analysis, % exp (calcd): Mo 54.27 (52.25), N 2.69 (2.77), P 1.63 (1.53), V 2.53 (2.52), C 0.5.

Mixed ammonium–cesium salts containing x cesium cations per heteropolyanion, noted as xCs ($x = 1$, 2, 2.7, 3, 3.2, 3.5), were prepared from the ammonium 1-vanado(V)-11-molybdophosphate. Exchange between ammonium and cesium cations was carried out by thermal treatment of $(NH_4)_4[PMo_{11}V^VO_{40}]$ impregnated by $CsNO_3$. A sample of $(NH_4)_4[PMo_{11}V^VO_{40}]$ (5 g, 2.47×10^{-3} mol) was impregnated at incipient wetness by a solution of $CsNO_3$ ($x \cdot 2.47 \times 10^{-3}$ mol in 2 mL of hot water). It was dried at 100 °C for 30 min and was then ground with a pestle and a mortar. This solid was heated in air flow (20 mL min^{-1}) using the following procedure: (a) the temperature was raised to 250 °C in 5 h (0.77 °C min^{-1}) and maintained for 20 h at this temperature; (b) the temperature was raised again to 300 °C at 0.21 °C min^{-1} and maintained for 3 h at this temperature; (c) the sample was cooled to room temperature. The sample 0 Cs is obtained by the same thermal treatment of the initial ammonium salt not impregnated by cesium nitrate.

For $Cs_4[PMo_{11}VO_{40}]$, two solutions were prepared: (A) The amount of 5.5 g of $H_4[PMo_{11}V^VO_{40}] \cdot 29H_2O$ was dissolved in 20 mL of dioxane. Then the heteropolyacid was neutralized by the addition of a lithium hydrogenocarbonate solution 0.5 M until pH $\approx$ 4.5 (19.2 mL). The lithium hydrogenocarbonate solution was obtained by bubbling CO_2 in a lithium hydroxide solution 0.5 M and it was titrated by HCl. (B) The amount of 1.863 g of cesium nitrate was dissolved in 20 mL of the water/dioxane mixture (1/1). Solution B was added dropwise to Solution A under stirring. An orange precipitate of cesium molybdovanadophosphate appeared after 1 min. The solid was collected by filtration through a fine frit, washed with cold water, and dried at room temperature for 2 days. Analysis, % exp (calcd): Mo 41.8 (42.1), Cs 21.46 (21.19), P 1.41 (1.23), V 1.91 (2.03), C < 0.3.

$(NH_4)_4[SiMo_{12}O_{40}]$ was obtained in two steps, first synthesis of the 12-molybdosilicic acid $H_4[SiMo_{12}O_{40}]$ as previously described [21], and then neutralization of this acid. The heteropolyacid was neutralized by an ammonium hydrogenocarbonate solution, 1.1 M, in water up to pH $\approx$ 4. The solution was then precipitated by NH_4Cl. The solid was collected by filtration through a fine frit, washed with cold water, and dried at room temperature. Analysis, % exp (calcd): Mo 55.34 (56.56), N 2.52 (2.75).

2.2. Characterizations of the solids

Nitrogen adsorption–desorption isotherms were obtained using a Micromeritics ASAP 2010 apparatus. The samples were evacuated at 150 °C for 2 h. Results were analyzed by the ASAP 2010 V3.00 program.

Density measurements were performed using a Micromeritics AccuPyc 1330 gas pycnometer (He).

Morphology of the solids was observed by scanning electron microscopy using a JEOL JSM-5800LV microscope. X-ray diffraction patterns (XRD) were recorded at room temperature with a Siemens D 5000 diffractometer using Cu-K_α radiation ($\lambda = 1.5418$ Å) and were fitted by means of the Socabim program PROFILE. Unit cell parameters were determined with the program DICVOL91 [22] and were refined by means of the program NBS*AIDS83 [23]. Rietveld refinements were undertaken by using the FullProf [24] program integrated in WinPLOTR [25] software. X-ray thermodiffractometry (XRTD) was performed in air in an Anton Paar HTK16 high-temperature device of a Siemens D 5000 diffractometer (θ–θ mode) using Co-K_α radiation ($\lambda = 1.7903$ Å), and equipped with a M Braun linear position sensitive detector (PSD). Samples were deposited directly on the heating platinum support connected to a thermocouple. Patterns were recorded from 30 to 610 °C every 20 °C, with a temperature ramp of 1.8 °C min^{-1}. The temperature was stabilized 2 min before measurements; each data collection lasted 570 s.

Thermogravimetry measurement (TGA) was carried out in air flow (60 mL min^{-1}) with a Perkin-Elmer electrobalance TGA-7 at a heating rate of 5 °C min^{-1} up to 600 °C. Differential Scanning Calorimetry (DSC) was carried out in air flow (60 mL min^{-1}) with a TA Instruments DSC 2010 at a heating rate of 5 °C min^{-1} up to 600 °C. Infrared spectra of KBr pellets were recorded on a Fourier Transform IR Nicolet 550 apparatus.

Solution ^{31}P NMR spectra were recorded on a Bruker AC 300 apparatus at 121.5 MHz. Chemical shifts are referenced to 85% H_3PO_4. Initial concentration in heteropolyanion is 6.5×10^{-2} mol L^{-1}.

2.3. Catalytic reaction

Oxidative dehydrogenation of IBA was studied under standard conditions in order to obtain structure–reactivity relationships. Catalytic reaction was carried out at 320 °C using a continuous flow pyrex microcatalytic reactor at atmospheric pressure. The feed gas consisted of 2% IBA, 5.2% O_2, 3.5% H_2O, and N_2 balance; total flow rate was 180 mL min^{-1}. The catalyst (0.3 g) was introduced in the reactor and the temperature of reaction was reached in 30 min in air flow (180 mL min^{-1}). All reaction products were analyzed by on-line gas-phase chromatography with molecular sieves 5 Å, Porapak Q, and AT 1200 with 1% H_3PO_4 columns. Carbon, oxygen, and hydrogen balances were in the range 90–100%. The catalytic performances were determined after 18 h of reaction.

3. Results

3.1. Synthesis and characterization of $(NH_4)_4[PMo_{11}VO_{40}]$

Ammonium or cesium 12-molybdophosphates or 1-vanado-11-molybdophosphates can be obtained by addition of ammonium or cesium chloride (nitrate) to the solution of the heteropolyacid and filtration of the solid. An alternative method is the addition of ammonium (cesium) carbonate in a stoichiometric amount and evaporation of water. In the first case, it is difficult to eliminate quantitatively the protons; salts of composition $M_{3-x}H_x[PMo_{12}O_{40}]$ ($x \sim 0.3$) or $(NH_4)_3H[PMo_{11}VO_{40}]$ are currently obtained [26]. In the second method, we experienced that the basicity of $CO_3{}^{2-}$ is enough to partially decompose the polyanions which are stable only in acidic aqueous solution. In order to avoid partial hydrolysis of the heteropolyanion [27], bases of lower strength can be used. Another way is to utilize mixed water/organic solvents such as water/dioxane since hydroorganic solvents are known to stabilize the heteropolyanions. Hydrogenocarbonate ion has been chosen to neutralize acidity. The stability of the anion $[PMo_{11}V^{V}O_{40}]^{4-}$ in water/dioxane v/v has been checked by ^{31}P NMR spectroscopy during the neutralization by $(NH_4)HCO_3$ (Fig. 1). The peak of $[PMo_{11}V^{V}O_{40}]^{4-}$ at −3.31 ppm does not vary until the neutralization (4 eq/HPA). It is only after the neutralization that other weak peaks appear (−0.26 ppm (8.1%), 0.58 ppm (7.3%), 2.07 ppm (11.1%), and 2.45 ppm (7.4%) for 6 eq of base/HPA). Therefore it is possible to neutralize quantitatively the heteropolyacid in this solvent without any decomposition. It can be pointed out that $(NH_4)_4[PMo_{11}VO_{40}]$ is soluble in the water/dioxane solvent and crystallization occurs only after complete neutralization of the acid. Only one signal at −3.41 ppm is observed on the ^{31}P NMR spectrum of $(NH_4)_4[PMo_{11}V^{V}O_{40}]$ after dissolution in a water/dioxane solvent. Elemental analysis of the crystals shows that neutral $(NH_4)_4[PMo_{11}VO_{40}]$ is effectively obtained.

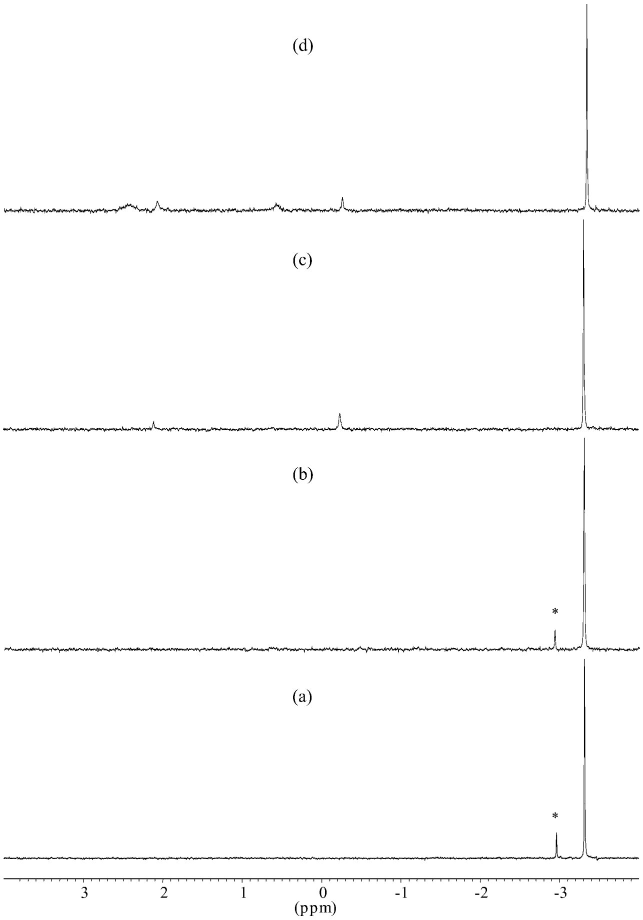

Fig. 1. NMR spectra following the neutralization of $H_4[PMo_{11}V^{V}O_{40}]$ by NH_4HCO_3 in water/dioxane (v/v): $H_4[PMo_{11}V^{V}O_{40}]$ (6.5×10^{-2} mol L^{-1}) (a), 4 eq of base/HPA (b), 5 eq of base/HPA (c), 6 eq of base/HPA (d) (the asterisk indicates the signal of trace of $[PMo_{12}O_{40}]^{3-}$).

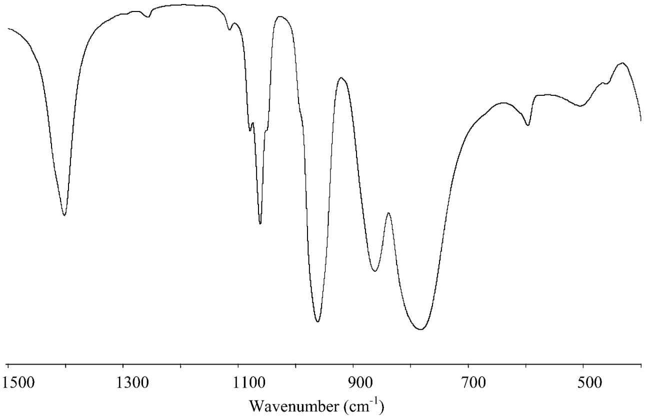

Fig. 2. Infrared spectrum of $(NH_4)_4[PMo_{11}V^VO_{40}]$.

The salt is composed of fine crystals (2 µm average diameter) forming aggregates and has a specific surface area of 16 $m^2\,g^{-1}$.

The IR spectrum of $(NH_4)_4[PMo_{11}V^VO_{40}]$ (Fig. 2) presents an intense band at 1062 cm^{-1} and two shoulders at 1051 and at 1079 cm^{-1}. As it is well known, such a splitting of the antisymmetric P–O vibration corresponds to the lowering of the symmetry of the central PO_4 tetrahedron to Cs symmetry due to the substitution of one Mo in $[PMo_{12}O_{40}]^{3-}$ by one vanadium atom. The other bands are classically observed in Keggin-type heteropolyanions [28] and are not modified by this weak change.

The X-ray diffraction pattern of $(NH_4)_4[PMo_{11}V^VO_{40}]$ is indexed with a cubic unit cell ($a = 11.6293(5)$ Å; space group $Pn\bar{3}m$) similar to that of $(NH_4)_3[PMo_{12}O_{40}]$ ($a = 11.6341(6)$ Å) [16]. The corresponding atomic coordinates of $(NH_4)_3[PMo_{12}O_{40}]$ [29] have been used as the starting model in the Rietveld refinement in which one molybdenum atom is substituted by one vanadium. A priori, this result raises a question since this compact structure can only accommodate three cationic positions for each heteropolyanion. For the location of the cation, two hypotheses have been considered: (1) as proposed by Berndt et al. a partial occupation of 3/4 for the anionic site is taken into account; (2) no anionic defaults are considered and some attempts to find an additional cation are undertaken. In order to increase the atomic contrast to eventually obtain clearer difference Fourier maps, the stoichiometric cesium salt $Cs_4[PMo_{11}V^VO_{40}]$ has also been prepared. Its X-ray diffraction pattern has been indexed with a slightly higher unit cell ($a = 11.7238(2)$ Å; space group $Pn\bar{3}m$). The results of Rietveld refinements (Table 1) are in favor of the first hypothesis and no additional cations are evident by difference Fourier calculation either in ammonium salt or in cesium compound.

Density measurements were performed for the ammonium $(NH_4)_4[PMo_{11}VO_{40}]$ and cesium $Cs_4[PMo_{11}VO_{40}]$ salts. The experimental values are respectively $\rho = 3.55$ and 3.22 $g\,cm^{-3}$. A very good agreement between experimental $\rho = 3.55$ $g\,cm^{-3}$ and calculated $\rho = 3.57$ $g\,cm^{-3}$ was obtained for $Cs_4[PMo_{11}VO_{40}]$ considering the presence of 6 Cs^+ (all positions) and only 1.5 $[PMo_{11}VO_{40}]^{4-}$ ($\frac{3}{4}$ positions) in the unit cell with the experimental parameter $a = 11.7238(2)$ Å. These values can be compared to the calculated value $\rho = 4.65$ $g\,cm^{-3}$ for 2 $Cs_4[PMo_{11}VO_{40}]$ in the unit cell. In the case of $(NH_4)_4[PMo_{11}VO_{40}]$, the calculated value is equal to 3.04 $g\,cm^{-3}$ if $\frac{3}{4}$ of the anionic positions are occupied whereas the value is equal to 3.97 $g\,cm^{-3}$ if all the anionic positions are occupied. The density of 3.22 $g\,cm^{-3}$ is rather in agreement with the anion-deficient model.

Table 1
Structural model indicators (R_B, R-Bragg factor; R_F, R-structure factor) of final Rietveld refinements with isotropic temperature factors (B_{iso}) of cations

Compound[a]	Crystal model indicators		Anionic occupancy	B_{iso} of N or Cs atoms
	R_B	R_F		
$(NH_4)_4[PMo_{11}V^VO_{40}]$ (a)	0.072	0.109	0.75	4.2(8)
	0.099	0.118	1[b]	0.4(8)
$(NH_4)_3H[PMo_{11}V^VO_{40}]$ (b)	0.101	0.077	0.75	4.4(9)
	0.107	0.08	1[b]	0.2(9)
$(NH_4)_{2.4}H_{1.6}[PMo_{11}V^VO_{40}]$ (c)	0.070	0.069	0.75	4.3(9)
	0.091	0.074	1[b]	−0.1(8)
$(NH_4)_{1.2}H_{1.8}[PMo_{11}V^VO_{40}]$ (d)	0.066	0.056	0.75	4.8(7)
	0.070	0.057	1[b]	0(7)
$Cs_4[PMo_{11}V^VO_{40}]$ (e)	0.062	0.071	0.75	4.36(9)
	0.096	0.095	1[b]	1.99(8)

[a] (a) and (e): initial compounds. (b), (c), and (d): $(NH_4)_4[PMo_{11}V^VO_{40}]$ treated at 220, 300, and 310 °C, respectively, in air flow and rehydrated in ambient atmosphere. Amount of ammonium cations determined by TG.

[b] Rietveld refinements with anionic and cationic occupancies of 1 have been undertaken in order to localize additional cations necessary for charge balance. These results are given for information.

3.2. Thermal behavior of the ammonium salt

Three weight losses are seen on the thermogravimetric curve of $(NH_4)_4[PMo_{11}VO_{40}]$ (Fig. 3, curve a) recorded

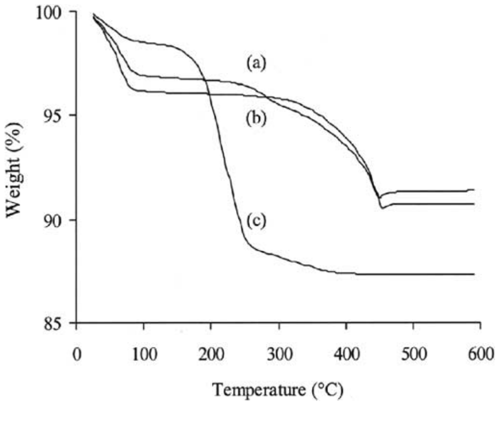

Fig. 3. Thermogravimetric curves recorded in air flow of $(NH_4)_4[PMo_{11}V^VO_{40}]$ (a), $(NH_4)_4[PMo_{11}V^VO_{40}]$ thermal treated in air flow at 220 °C (b), and $(NH_4)_4[PMo_{11}V^VO_{40}]$ impregnated by 3 $CsNO_3$ (c).

in air flow. The first one, between 25 and 100 °C, is attributed to three adsorbed water molecules and leads to the formation of anhydrous salt [29]. The second one, between 200 and 300 °C, and the third one, between 300 and 500 °C, are not well separated; the total loss corresponds to 118 $\mathrm{g\,mol^{-1}}$. Considering the presence of 0.5% of carbon shown by elemental analysis and under presumed dioxane form (17 $\mathrm{g\,mol^{-1}}$) the corrected total loss corresponds to 101 $\mathrm{g\,mol^{-1}}$, in good agreement with the value 104 $\mathrm{g\,mol^{-1}}$ calculated for decomposition into oxides of $(NH_4)_4[PMo_{11}VO_{40}]$.

A thermal treatment of the initial salt was performed in air flow at 220 °C. Elemental analysis of the treated solid indicates 3 NH_4^+ per mole and only one weight loss of 89 $\mathrm{g\,mol^{-1}}$ is seen at temperatures higher than 280 °C on the TG curve (Fig. 3, curve b). It is assigned to $3NH_3 + 2H_2O$ corresponding to the decomposition of the acidic salt $(NH_4)_3H[PMo_{11}VO_{40}]$ into oxides (theoretical value 87 $\mathrm{g\,mol^{-1}}$). The first weight loss observed with the initial salt after 200 °C is thus attributed to the formation of the acidic salt $(NH_4)_3H[PMo_{11}VO_{40}]$.

The DSC curve (Fig. 4, curve a) can be compared with the weight losses seen on the TG curve. The first peak at 60 °C is endothermic and corresponds to the loss of hydration water molecules. The second peak at 265 °C is strongly exothermic and can likely be associated to the weight loss recorded between 200 and 300 °C. The exothermic peaks above 440 °C correspond to the loss and, probably, oxidation of the remaining ammonia molecules and to oxide crystallization. Otherwise, the exothermic peak at 265 °C is not observed on the DSC curve of the heated salt at 220 °C which has already lost one ammonia molecule (Fig. 4, curve b).

In order to understand the origin of the exothermic transformation at 265 °C, the ammonium 12-molybdosilicate $(NH_4)_4[SiMo_{12}O_{40}]$ was prepared by neutralization of the acid by NH_4HCO_3 in water. This compound has also the same structure as the cubic $(NH_4)_3[PMo_{12}O_{40}]$ salt, with $a = 11.6128(3)$ Å; space group $Pn\bar{3}m$, like $(NH_4)_4[PMo_{11}V^VO_{40}]$ salt. In this salt, the anionic charge results from the substitution of the central P^V by Si^{IV} instead of the substitution of one Mo^{VI} by one V^V. The thermogravimetric curve recorded in air flow shows three weight losses as in the case of $(NH_4)_4[PMo_{11}V^VO_{40}]$. The first one, between 25 and 100 °C, is attributed to eight water molecules and leads to the formation of the anhydrous salt. The second one, between 200 and 300 °C, and the third one, between 300 and 450 °C, are not well separated; the total loss corresponds to 103 $\mathrm{g\,mol^{-1}}$.

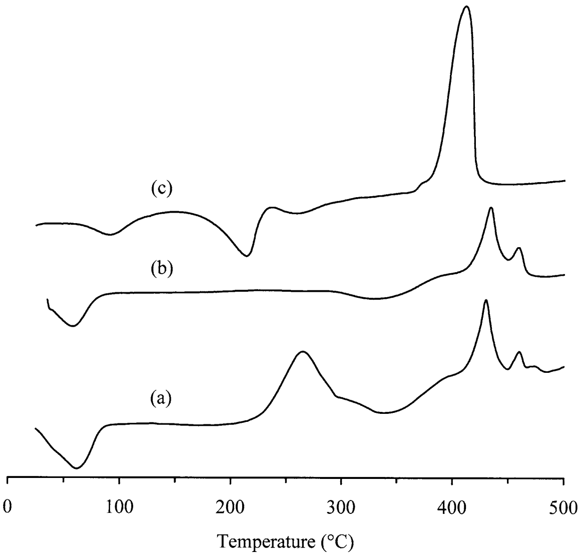

Fig. 4. Differential Scanning Calorimetry curves recorded in air flow of $(NH_4)_4[PMo_{11}V^VO_{40}]$ (a), $(NH_4)_4[PMo_{11}V^VO_{40}]$ heated in air flow at 220 °C (b), and $(NH_4)_4[SiMo_{12}O_{40}]$ (c).

A thermal treatment of the initial salt was performed in air flow at 220 °C and then up to 600 °C. The first loss at 220 °C corresponds to 1 NH_3 per mole and the second weight loss of 89 $\mathrm{g\,mol^{-1}}$ at temperatures higher than 270 °C is assigned to $3NH_3 + 2H_2O$ and corresponds to the decomposition of the acidic salt $(NH_4)_3H[SiMo_{12}O_{40}]$ into oxides.

The DSC curve of $(NH_4)_4[SiMo_{12}O_{40}]$ shows two endothermic peaks at 90 and 215 °C and an exothermic peak at about 400 °C, but not the strong exothermic peak at 265 °C (Fig. 4, curve c) observed on the DSC curve of $(NH_4)_4[PMo_{11}V^VO_{40}]$. In conclusion, the exothermic peak at 265 °C must be correlated to the presence of a vanadium atom in the Keggin structure and to the departure of the first ammonia molecule.

Evolution of the X-ray pattern of $(NH_4)_4[PMo_{11}V^VO_{40}]$ with temperature is shown in Fig. 5. The cubic phase is observed up to 410 °C and then the peaks of molybdenum oxide appear. But a slight shift of all diffraction lines toward smaller θ is observed above 250 °C; it corresponds to an increase of the lattice parameter with temperature.

3.3. *Characterization of the treated ammonium salt*

X-ray diffractometry and TG measurement reveal that ammonia molecules are eliminated whereas the cubic structure is maintained. Could all ammonium cations be released to form the acid with the same cubic structure previously depicted by Berndt et al.? Thermal treatments of the initial salt $(NH_4)_4[PMo_{11}V^VO_{40}]$ have been performed (for several days) at different temperatures (220, 280, 290, 300, and 310 °C) in air flow and the samples have been characterized by X-ray diffraction, IR spectroscopy, and thermal analysis after rehydration in ambient atmosphere.

The amount of ammonium cations decreases as temperature increases, showing that ammonia is progressively eliminated. The infrared spectra show that the relative intensity of the ammonium vibration decreases as ammonia is eliminated and that the shoulders of the P–O vibration at 1051 and at 1079 $\mathrm{cm^{-1}}$ are present but less resolved than for the initial salt. On the contrary, the other characteristic bands of the heteropolyanion are not modified up to 300 °C, showing that the Keggin structure is kept. The X-ray diffraction patterns

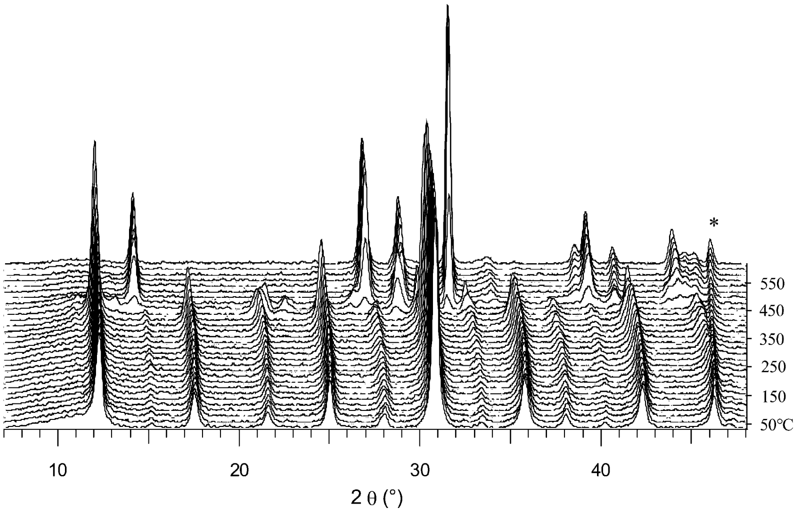

Fig. 5. Evolution of the XRD patterns with temperature from 30 °C up to 610 °C recorded every 20 °C for $(NH_4)_4[PMo_{11}V^VO_{40}]$ (the asterisk indicates spirious diffraction line of the sample holder).

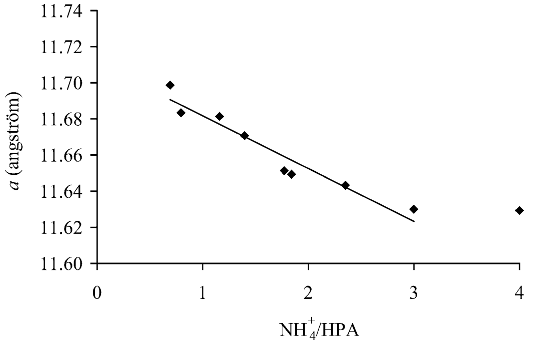

Fig. 6. Evolution of the lattice parameter in function of the amount of remaining ammonium cations per heteropolyanion after thermal treatments of the initial salt $(NH_4)_4[PMo_{11}V^VO_{40}]$ at different temperatures (220 to 310 °C) in air flow.

of the treated samples have all been indexed with a cubic unit cell (space group $Pn\bar{3}m$). As the amount of ammonium decreases, the lattice parameter increases (Fig. 6). Rietveld refinements have been performed on treated samples at different temperatures (Table 1). Since X-ray scattering factors of oxygen and nitrogen are close, we did not consider a statistic occupation of the cationic position by NH_4^+ and H_3O^+. In the hypothesis of full occupation of cationic and anionic sites, difference Fourier maps did not allow the location of additional H_3O^+ and no site with coherent hydrogen bonds distances was found for hydronium in this compact structure.

It is not possible to eliminate the four ammonia molecules at 300 °C whatever the lengthening of thermal treatment, and a limiting composition $(NH_4)_{0.8}H_{3.2}[PMo_{11}VO_{40}]$ has been obtained without any modification of the Keggin structure and of the cubic lattice. Indeed, additional peaks are observed on the X-ray pattern. After a long treatment at 310 °C, additional peaks are observed on the X-ray pattern and a new band at 1035 cm^{-1} is present on the IR spectrum. This new band has been previously correlated with the presence of vanadium species out of the Keggin structure [10]. New peaks observed by X-ray diffraction could not be attributed to a known phase. All this suggests a transformation of the Keggin anion $[PMo_{11}VO_{40}]^{4-}$ at this temperature.

The specific surface area of the initial ammonium salt is low (16 $m^2\,g^{-1}$) but a large increase to 143 $m^2\,g^{-1}$ occurs when the first ammonia molecule is eliminated in air at 220 °C; it increases only slightly at higher temperatures (173 $m^2\,g^{-1}$ for 2.4 NH_4^+).

3.4. Preparation and characterization of mixed ammonium–cesium salts

The mixed ammonium–cesium salts have been obtained by solid-state cationic Cs^+/NH_4^+ substitution which occurs during a thermal treatment of the ammonium salt impregnated by cesium nitrate at incipient wetness [16]. The exchange is promoted by the decomposition of ammonium nitrate at temperatures higher than 210 °C. The thermogravimetric curves of $(NH_4)_4[PMo_{11}V^VO_{40}]$ (a) and of the $(NH_4)_4[PMo_{11}V^VO_{40}] + 3CsNO_3$ mixture (c) are shown in Fig. 3. The weight loss observed at temperature higher than 180 °C on curve c is attributed to the decomposition of ammonium nitrate. It can be seen that a temperature as high as 300 °C is needed to obtain a quantitative decomposition of NH_4NO_3. The treatment was then performed in two steps, first at 250 °C in order to eliminate more than 80% of the ammonium nitrate and then at 300 °C in order to complete the cationic exchange. Under these conditions, no decomposition of the heteropolyanion was observed as shown by infrared spectroscopy and only one cubic phase was seen by X-ray diffraction.

The infrared spectra of the solids xCs are given in Fig. 7. For all samples, the shoulders of the ν_{as} P–O vibration at 1051 and at 1079 cm^{-1} are present but less resolved than for the initial $(NH_4)_4[PMo_{11}V^VO_{40}]$ ammonium salt. The relative intensity of the δ N–H vibration at 1410 cm^{-1} decreases

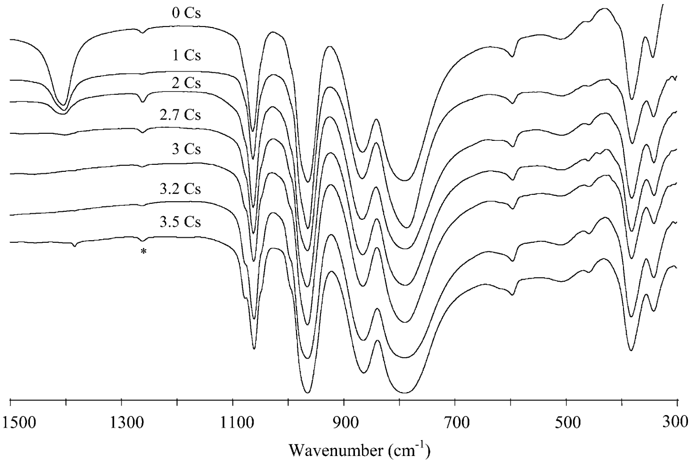

Fig. 7. Infrared spectra of the xCs solids obtained after thermal treatment in air flow (the asterisk indicates a KBr impurity).

Table 2
Amount of ammonium cations per heteropolyanion in the xCs samples obtained after thermal treatment in air flow before and after use in reaction determined by elemental analysis (a) and estimated by the losses between 250 and 600 °C measured by thermogravimetric analysis (b)

Compounds	0 Cs	1 Cs	2 Cs	2.7 Cs	3 Cs	3.2 Cs	3.5 Cs
Before reaction							
(a)	3.1	1.07	0.3	Trace	0	0	0
(b)	3	1.65	0.58	0.19	0.06	[a]	[a]
After reaction							
(a)	0.75	0.38	0	0	0	0	0
(b)	0.5	[a]	[a]	[a]	[a]	[a]	[a]

[a] Under the limit of analysis.

when x increases from 1 to 3 and, for $x = 3$, this band disappears. For $x = 3.5$, a fine band at 1385 cm^{-1} appears and corresponds to an excess of cesium nitrate. Therefore only three on the four ammonium cations can be replaced by cesium cations. Thermogravimetric analysis and elemental analysis show that the amount of ammonium cations is always smaller than the expected amount (Table 2). This shows that decomposition of ammonium cations occurs during the cationic Cs^+/NH_4^+ exchange. The X-ray diffraction patterns of all samples have been indexed in the cubic symmetry. The lattice parameter increases with x up to about 2 and remains constant for higher x values (Fig. 8). Nevertheless exchange is confirmed for $2 \leqslant x \leqslant 3$ by some important variations of several line intensities on diffraction patterns, especially for (200) and (220) reflections which decrease and vanish for $x = 3$ and for (211) and (332) which increase up to $x = 3$.

3.5. Catalytic behavior

In the first 5 h of reaction the conversion and the selectivity to MAA improve and then a slow decrease of the conversion but a little improvement of the selectivity to MAA are observed for $x \leqslant 3$. A quasi steady state is reached and the catalytic activity of the xCs samples is reported in Fig. 9. The yield of MAA changes only slightly for $0 \leqslant x < 3$ (48.2 to 45.6%) but a drastic evolution of the catalytic behavior occurs between 3 and 3.2 Cs: the conversion of IBA and the selectivity to MAA fall down sharply while acetone becomes the major product. Propene is formed in a very small quantity for $x = 3$ and the proportion of CO and CO_2 increases hereafter.

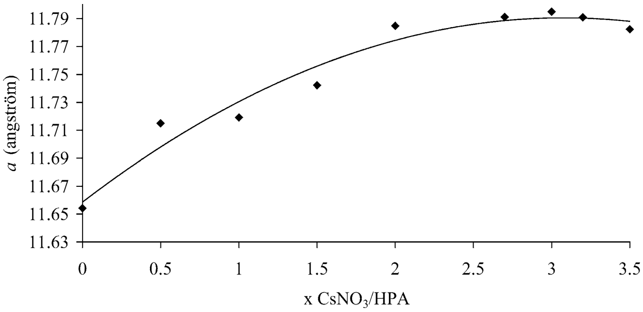

Fig. 8. Variation of the unit cell parameter of cubic phase of the xCs samples obtained after thermal treatment in air flow versus the amount of impregnated $CsNO_3$.

Infrared spectra of the catalysts after use in reaction are given in Fig. 10. For $x < 2$, the shoulder of the P–O vibration at 1062 cm^{-1} disappears, this band becomes symmetric, and a small band presumably due to cationic vanadyl species [10] is observed at 1035 cm^{-1}. When $x > 2$, the shoulders of the P–O vibration are still present after reaction and are better defined for increasing x values. The relative N–H vibration intensity decreases to disappear for $x = 2$.

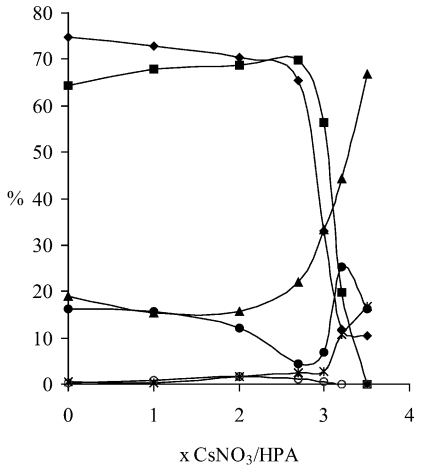

Fig. 9. Catalytic performance after 18 h on reaction of the treated ammonium salt (0 point) and of the xCs samples (◆, IBA conversion; selectivity to MAA, ■; acetone, ▲; propene, ●; acetic acid, ○; CO$_x$ ★).

The remaining amount of ammonium cation has been calculated for each sample by thermogravimetry and elemental analysis (Table 2). The release of ammonia in the conditions of reaction is very important; xCs samples with $x \geqslant 2$ are free of ammonium cations after reaction. A new large band at 628 cm^{-1}, characteristic of reduced molybdenum oxide [18], appears when $x < 2$ and its relative intensity decreases when x increases. The samples are deep blue when $x < 2.7$. For $x = 2.7$ and 3, the samples display a pale green color.

4. Discussion

4.1. Structure of the catalysts and thermal behavior

Structures of heteropolyacids and salts are strongly dependent on the nature of the counterions and on the amount of hydration water molecules. Highly hydrated acids are triclinic but salts obtained with large alkaline cations (K$^+$, Rb$^+$, Cs$^+$), less hydrated, are cubic. Recently, it has been shown by Berndt et al. [19] that, in addition to the triclinic phase, a small fraction of thin crystals of the acid has the cubic $Pn\bar{3}m$ structure as well and that all the members of the series of salts Cs$_x$H$_{4-x}$[PMo$_{11}$VO$_{40}$] $\cdot n$H$_2$O ($x = 2$–4) have this cubic structure.

The ammonium cation has been chosen in this study because (i) it is similar to the hydrated proton (H$_3$O$^+$ or H$_2$O$_5$$^+$), (ii) its decomposition by heating treatment leads, after rehydration of the solid in ambient air, to hydrated protons; (iii) it can be substituted by cesium by a solid-state thermal treatment in presence of cesium nitrate.

In water/dioxane v/v solution, the neutralization of the acid by (NH$_4$)HCO$_3$ is complete without partial decomposition of the heteropolyanion and before the crystallization occurs. In consequence, the true neutral salt (NH$_4$)$_4$[PMo$_{11}$VO$_{40}$] is obtained. Whereas the anionic charge of the heteropolyanion increases by substitution of one molybdenum atom by one vanadium, a cubic unit cell similar to that of (NH$_4$)$_3$[PMo$_{12}$O$_{40}$] is found. The Rietveld refinement converged to better crystal model indicators for an anionic occupation of 3/4 and thermal factors of nitrogen atoms are also more realistic (Table 1). In the case of full occupancy of the cationic and anionic sites, no additional cations could be located by difference Fourier maps even for the Cs$_4$[PMo$_{11}$VO$_{40}$] sample. Therefore, these results confirm the anionic default proposed by Berndt et al. for cesium salt.

Could this conclusion be applied to other four ammonium or cesium salts? The 12-molybdosilicate anion has the same negative charge as the 1-vanado-11-molybdophosphate and the ammonium salt (NH$_4$)$_4$[SiMo$_{12}$O$_{40}$] has been obtained by the same method. As expected, these two neutral ammonium salts are isostructural with about the same unit cell parameter. Therefore, it seems to be possible to extend the amazing conclusion that the cubic structure could accommodate four monovalent cations by an anionic default [19]. But for five ammonium cations, the symmetry is different [17].

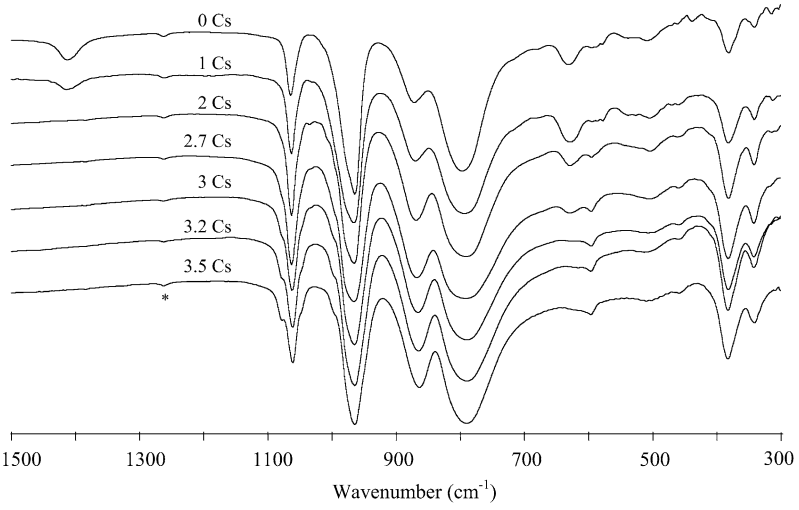

Fig. 10. Infrared spectra of xCs samples after use in reaction (the asterisk indicates a KBr impurity).

The thermal treatment of $(NH_4)_4[PMo_{11}VO_{40}]$ at 220 °C in air flow leads, as expected from the thermogravimetric curve, to the acidic salt $(NH_4)_3H[PMo_{11}VO_{40}]$. So, decomposition of one of the four NH_4^+ cations occurs at relatively low temperature and would lead to a more stable salt in which, following the model of Berndt, both cationic and anionic sites are totally occupied. Rietveld refinements of the diffraction patterns of $(NH_4)_4[PMo_{11}VO_{40}]$ and treated samples are comparable (Table 1). The results are in better agreement with the model of anionic vacancies with all occupied cationic positions. Taking into account that no difference could be observed between NH_4^+ and H_3O^+ by powder X-ray diffraction, this result is in agreement with a substitution of a NH_4^+ by a proton during thermal treatment; this proton is then rehydrated and is in the form of H_3O^+. It could be concluded that the anionic default is conserved whereas it is not in agreement with the model proposed by Berndt et al. for acidic cesium salts. Furthermore, this model is valid for all treated samples with variable amount of remaining ammonium.

The important exothermic phenomenon observed on the DSC curve at about 265 °C is very likely due to the oxidation of the released ammonia molecule to nitrogen and/or nitrogen oxides. Interestingly, no exothermic phenomenon is observed under the same conditions with $(NH_4)_4[SiMo_{12}O_{40}]$ even if the acidic salt $(NH_4)_3H[SiMo_{12}O_{40}]$ is obtained under the same experimental conditions. This means that, in this case, the released ammonia molecule is not oxidized. This result clearly shows that the vanadium atom in the Keggin structure enhances strongly the oxidizing ability of the polyoxometalate which is thus able to catalyze the oxidation of NH_3 by oxygen at 220 °C.

A series of salts $(NH_4)_{4-y}H_y[PMo_{11}VO_{40}]$ has been obtained with $0 < y < 3.2$ by long thermal treatments (several days) of the ammonium salt performed in air flow at temperatures ranging from 220 to 300 °C. It has not been possible to decompose quantitatively the ammonium cations in order to obtain the cubic acid $H_4[PMo_{11}VO_{40}]$ because a partial transformation of the heteropolyanion occurs at higher temperature. The important point is that the cubic phase is maintained whatever the composition. The unit cell parameter increases quite linearly as the ammonium amount decreases, below 3 NH_4^+/HPA, suggesting that ammonium cations and hydrated protons are statistically distributed in the cationic sites (Fig. 6). Extrapolation of the unit cell parameter for $x = 0$ gives a value of 11.71 ± 0.01 Å which can be compared with the value obtained by Berndt et al. (12.0 ± 0.4 Å) from electron diffraction patterns of the small amount of the acid which is cubic.

An important consequence of the progressive loss of ammonia is the increase of the specific surface area from 16 $m^2\,g^{-1}$ for $(NH_4)_4[PMo_{11}VO_{40}]$ (crystalline sample) to 143 $m^2\,g^{-1}$ for $(NH_4)_3H[PMo_{11}VO_{40}]$ (fine powder) showing that texture of the solid is strongly modified. Such a high specific surface area has also been observed for $Cs_3H[PMo_{11}VO_{40}]$ [19] and, in this study, for $Cs_4[PMo_{11}VO_{40}]$, which develops a specific surface area of 150 $m^2\,g^{-1}$ (after evacuation at 200 or 350 °C for 2 h).

4.2. Exchange Cs^+/NH_4^+

It has been proven that cesium counterions change physical and chemical properties of the heteropolyanion such as stability, porosity, acid strength, and oxidizing ability [1] which are relevant for an application in heterogeneous catalysis. Preparation of mixed cesium–ammonium salts $(NH_4)_{4-x}Cs_x[PMo_{11}VO_{40}]$ has been tempted by a solid-state Cs^+/NH_4^+ exchange starting from the ammonium salt. Figs. 3 and 7 show that the driving force of the solid-state exchange between ammonium and cesium cations is the decomposition of ammonium nitrate and that a temperature of 300 °C is sufficient in order to obtain a quantitative elimination of NH_4NO_3. Apparition of a small band at 1385 cm^{-1} only for $x > 3$ shows that nitrate is really eliminated for lower x values and thus that the cationic Cs^+/NH_4^+ exchange is quantitative.

Up to about $x = 2$ the Cs^+/NH_4^+ substitution gives rise to an increase of the unit cell parameter which remains constant for higher x values (Fig. 8). Actually, at the temperature needed for the cationic exchange, decomposition of ammonium cations associated to a loss of ammonia occurs simultaneously with the Cs^+/NH_4^+ exchange. The exact composition of the solid depends on the relative rates of ammonium decomposition and cationic exchange. As previously seen, the first ammonium cation is decomposed very quickly at temperatures of 250 and 300 °C required for the exchange and it results that no more than three ammonium cations can be expected to be substituted by cesium cations. But substitution of ammonium by either hydrated protons or cesium cations gives rise to an increase of the lattice parameter. So, the increase of the lattice parameter up to $x = 2$ is very likely due to substitution of ammonium cations by both cesium and hydrated protons and, for $x > 2$, since no ammonium cations remain after the thermal treatment, the lattice parameter is not strongly dependent on the value of x in samples. This is in agreement with the values of 11.804, 11.807, and 11.785 Å obtained for $x = 2$, 3 and 4, respectively, with acidic salts obtained by the precipitation method [19].

4.3. Reactivity

Catalytic behavior is another probe which can give information on the exact compositions of the solids. For low x values, the catalysts have a deep blue color after reaction, showing that heteropolyanion is partially reduced at the steady state and thermogravimetric analysis shows that ammonia is lost during the reaction (Table 2). Moreover, the absence of the shoulder of the P–O vibration and a new band at 1035 cm^{-1} suggests that vanadium atoms have moved to a cationic position [10]. On the other hand, partial decomposition of the heteropolyanions into partly reduced molybdenum oxide is proven by the observation of a large band at

625 cm^{-1}. Increasing amounts of cesium limits the reduction and the decomposition since the relative intensity of the 625 cm^{-1} band decreases.

The evolution of the catalytic performances in the first hours of reaction could be due to the change of the catalyst composition under the reactive steam. Selectivities and conversion reach a quasi steady state; thus, they are reported after 18 h of reaction.

The drastic variation of the catalytic behavior for $x \approx 3$ has been previously observed [5,18]. For $x > 3$ the composition of the polyanion is not modified after use since infrared spectra are unchanged (Figs. 7 and 10), but the catalysts are inactive for MAA production. Lee et al. explain the selective formation of acetone by the surface basicity caused by Cs species (possibly oxides or carbonates). Another explanation can be proposed without the requirement of new basic sites. Actually, the yield of acetone is approximately the same before and after $x = 3$ and is likely due to the basicity of the oxygen atoms of the heteropolyanion which could be increased by the presence of cesium [30]. The high selectivity in acetone can mainly be attributed to the fall of the rate of formation of MAA and propene.

Before $x = 3$, high catalytic activity is observed whatever the x value, whereas the composition of the initial or used catalyst varied. Such a behavior is obtained in the very similar ammonium–cesium salts obtained from the reduced $(NH_4)_5[PMo_{11}V^{IV}O_{40}]$ [18]. The drastic fall of the catalytic behavior occurring between 3 and 3.2 Cs can be explained by the nonpresence of small amounts of Lewis acid sites on the surface. It must be noted that IR spectra of the used catalysts are identical for each x value of both series. Indeed, conditions of reaction have induced reduction and nearly the same compounds are obtained at the steady state.

5. Conclusion

Stoichiometric ammonium or cesium salts of $[PMo_{11}VO_{40}]^{4-}$ or $[SiMo_{12}O_{40}]^{4-}$ have been prepared and they can display a cubic $Pn\bar{3}m$ structure. Rietveld refinements are improved by attribution of a 3/4 occupancy factor for the anionic position for $(NH_4)_4[PMo_{11}VO_{40}]$ and $Cs_4[PMo_{11}VO_{40}]$ as it was already reported for the cesium salt.

Cubic mixed acidic ammonium salts $(NH_4)_{4-y}H_y[PMo_{11}VO_{40}]$, $0 < y < 3.2$ have been obtained by air thermal treatment of the ammonium salt. Their unit cell parameter increases as the amount of ammonium decreases.

The solid-state exchange of Cs^+/NH_4^+ from $(NH_4)_4[PMo_{11}V^{V}O_{40}]$ occurs simultaneously with an elimination of ammonia. Thus no more than 3 Cs cations could be exchanged. The catalytic behavior of these salts is very similar to those of the mixed Cs^+/NH_4^+ salts issued from $(NH_4)_5[PMo_{11}V^{IV}O_{40}]$. The initial state of vanadium seems to have little influence. Indeed, conditions of reaction have induced reduction and transformation of the catalysts leading to nearly the same compounds.

References

[1] M. Misono, Chem. Commun. (2001) 1141.
[2] G.P. Schindler, T. Ui, K. Nagai, Appl. Catal. A 206 (2001) 183.
[3] F. Cavani, A. Tanguy, F. Trifirò, M. Koutrev, J. Catal. 174 (1998) 231.
[4] M. Misono, N. Mizuno, T. Komaya, in: Proceedings, 8th International Congress on Catalysis, Berlin, Vol. 5, Dechema, Frankfurt-am-Main, 1984, p. 487.
[5] K.Y. Lee, S. Oishi, H. Igarashi, M. Misono, Catal. Today 33 (1997) 183.
[6] N. Mizuno, M. Tateishi, M. Iwamoto, J. Catal. 163 (1996) 87.
[7] N. Mizuno, H. Yahiro, J. Phys. Chem. B 102 (1998) 437.
[8] J.B. Black, N.J. Claydon, P.L. Gai, E.M. Serwicka, J. Catal. 106 (1987) 1.
[9] M. Langpape, J.M.M. Millet, U.S. Ozkan, M. Boudeulle, J. Catal. 181 (1999) 80.
[10] E. Cadot, C. Marchal, M. Fournier, A. Tézé, G. Hervé, in: M.T. Pope, A. Müller (Eds.), Polyoxometalates, Kluwer Academic, Dordrecht, 1994, p. 315.
[11] Th. Ilkenhans, B. Herzog, Th. Braun, R. Schlögl, J. Catal. 153 (1995) 275.
[12] C. Marchal-Roch, R. Bayer, J.F. Moisan, A. Tézé, G. Hervé, Top. Catal. 3 (1996) 407.
[13] J.K. Lee, J. Melsheimer, S. Berndt, G. Mestl, R. Schlögl, K. Köhler, Appl. Catal. A 214 (2001) 125.
[14] L. Marosi, G. Cox, A. Tenten, H. Hibst, J. Catal. 194 (2000) 140.
[15] L. Marosi, C. Otero Areán, J. Catal. 213 (2003) 235.
[16] C. Marchal-Roch, N. Laronze, R. Villanneau, N. Guillou, A. Tézé, G. Hervé, J. Catal. 190 (2000) 173.
[17] C. Marchal-Roch, N. Laronze, N. Guillou, A. Tézé, G. Hervé, Appl. Catal. 199 (2000) 33.
[18] C. Marchal-Roch, N. Laronze, N. Guillou, A. Tézé, G. Hervé, Appl. Catal. 203 (2000) 143.
[19] S. Berndt, D. Herein, F. Zemlin, E. Beckmann, G. Weinberg, J. Schütze, G. Mestl, R. Schlögl, Ber. Bunseges. Phys. Chem. 102 (1998) 763.
[20] P. Courtin, Rev. Chim. Min. 8 (1971) 75.
[21] R. Massart, Ann. Chim. 3 (1968) 507.
[22] A. Boultif, D. Louër, J. Appl. Crystallogr. 24 (1991) 987.
[23] A.D. Mighell, C.R. Hubbard, J.K. Stalik, NBS*AIDS80: A Fortran Program for Crystallographic Data Evaluation., Nat. Bur. Stand. (US), Technol. Note No 1141, 1981. NBS*AIDS83 is an expanded version of NBS*AIDS80.
[24] J. Rodriguez-Carvajal, in: Collected Abstract of Powder Diffraction Meeting, Toulouse, 1990, p. 127.
[25] T. Roisnel, J. Rodriguez-Carvajal, Mater. Sci. Forum 378-381 (2001) 118.
[26] J.G. Highfield, J.B. Moffat, J. Catal. 98 (1986) 245.
[27] L. Pettersson, in: M.T. Pope, A. Müller (Eds.), Polyoxometalates, Kluwer Academic, Dordrecht, 1994, p. 27.
[28] C. Rocchiggioli-Deltcheff, R. Thouvenot, R. Franck, Spectrochim. Acta 32 A (1976) 587.
[29] J.C.A. Boeyens, J.G. McDougal, J. van Smit, J. Solid State Chem. 18 (1976) 191.
[30] P. Moriceau, A. Lebouteiller, E. Bordes, P. Courtine, Phys. Chem. Chem. Phys. 1 (1999) 5735.